Analysis of High-Frequency Resistance in Transformers

Kazuhiko Sakakibara and Naoki Murakami

NTT Applied Electronics Laboratories
3-9-11, Midori-cho, Musashino-shi, Tokyo, 180 Japan

ABSTRACT

An accurate, analytical method is proposed for calculating the lead and winding high-frequency resistance of complex transformer constructions. High-frequency resistance is derived from the resulting matrix system equations, common to the leads and windings. The effect of eddy currents in the leads is confirmed by theoretical results. The high-frequency resistances of three winding arrangements are compared, and from this results, a winding geometry that reduces winding high-frequency resistance is derived.

INTRODUCTION

With the rise of switching frequency in switching power supplies, skin and proximity effects have become important considerations when calculating copper loss in transformers [1-3].

The basis of these research in this area is the study by Dowell [1], which examines a transformer whose windings carry identical current. However, this approach is not directly applicable to transformer winding layers that are connected in parallel, since the current in the windings is not equal. Also, the Dowell research deals only with winding resistance.

This paper discusses a numerical procedure which solves the matrix system equation, and derives exact analytical expressions for calculating the lead and winding high-frequency resistance in transformers. This method enables to calculate accurate resistance of complicated winding geometries.

TRANSFORMER CONFIGURATION

Figure 1 shows the basic configuration of a high-frequency transformer, which consists of magnetic core, leads, and windings. As frequency increases, additional losses occur in the leads and windings due to eddy currents induced in the conductors by the alternating magnetic field. The leads and windings are connected in series, therefore, the high-frequency resistance of the transformer Rt is

$$Rt = R_\ell + Rw \qquad (1)$$

where R_ℓ is the lead resistance and Rw is the winding resistance.

The goal of this study is to provide methods to calculate R_ℓ and Rw.

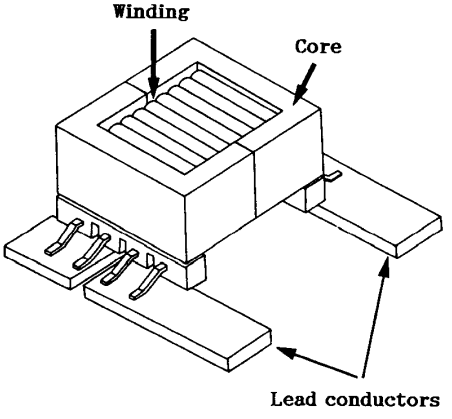

Fig. 1. Construction of transformer with lead conductors.

Since the mutual impedance of any two parallel leads can be expressed fully in terms of the the mutual impedance between various leads, it will suffice to discuss the fundamental configuration of two leads, I and II, in Fig. 2. The cross-sectional shape of each lead is uniform, but the cross-sectional shapes and areas of different leads need not be equal.

To create the lead models, each lead is represented by subconductors, which are correspondingly enable the resistance, and the mutual and self inductance to be described and

CH2721-9/89/0000-0618 $1.00 © 1989 IEEE

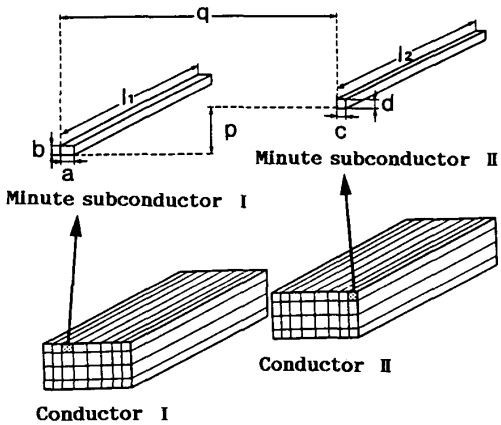

Fig. 2. Arrangement of lead conductors.

calculated.

Transformer windings constructed of primary and secondary windings can be approximated by infinitely long solenoids. The losses in any layer can be calculated if the winding arrangements and the magnetic field are known.

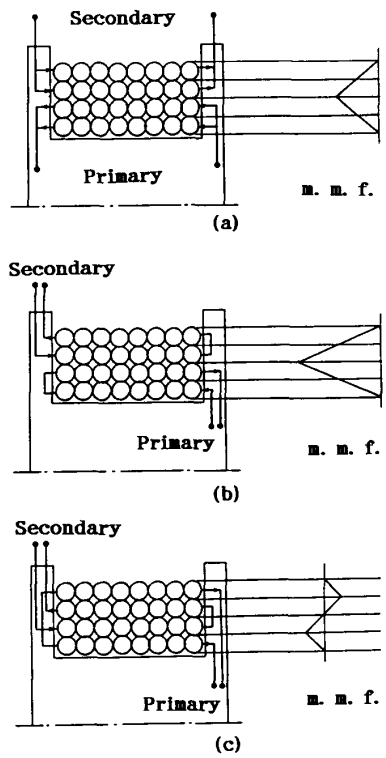

Fig. 3. Winding cross sections and m. m. f. diagrams.
(a) Multilayer pile winding. (b) Normal winding.
(c) Sectionized winding.

Figure 3 shows some typical winding arrangements and the corresponding m. m. f. diagrams. The high-frequency resistance of leads and windings are analyzed in the following section.

LEAD RESISTANCE

In this section, the analytical expressions are determined by which can be calculated high-frequency lead resistance.

List of symbols

Definitions of symbols used here are as follows.

a, b, c, d: Mesh widths of each minute subconductor
l_1, l_2: Lengths of lead I and lead II
p: Horizontal distance between subconductors
q: Vertical distance between subconductors
ω: Angular frequency
μ_o: Permeability of free space
ρ: Resistivity of the conductor material
δ: Skin depth ($= \sqrt{\frac{2\rho}{\omega \mu_o}}$)
n: Number of subconductors in lead I
m: Number of subconductors in lead II
$i_1 \sim i_{n+m}$: Complex currents of each subconductor
e_1, e_2: Complex voltage drops of lead I and lead II
I_1, I_2: Input or output current of the lead

Analysis

The new analytical method entails dividing leads into minute subconductors, as shown in Figure 2, and replacing each subconductor with its corresponding representation, as shown in Figure 4. Here each subconductor is shown with its associated resistance, and mutual and self inductance. The mutual inductance for each subconductor is calculated from the following equation [4] .

$$M_{ij} = \frac{\mu_o}{4\pi\, abcd} \sum_{i=1}^{4} \sum_{j=1}^{4} \sum_{k=1}^{4} [(-1)^{i+j+k+1} f(x_i, y_j, z_k)] \quad \text{-----(2)}$$

In this equation, $f(x_i, y_j, z_k)$ is a function of three independent variables. The variables of x_i, y_j and z_k are listed in Table 1. The function $f(x_i, y_j, z_k)$ is given in the Appendix A.

The self inductance for each subconductor is given again by Eq. (2), but in this case, the distances are p=0 and q=0.

The resistance for each subconductor is calculated from

$$r_i = \rho \frac{l_i}{A_i} \qquad (3)$$

where l_i is the length and A_i is the area of each subconductor. Using these expressions, the subconductor characteristics can be expressed in matrix form by

$$[Z]\ \{i\} = \{e\} \qquad (4)$$

where

$$[Z] = \begin{bmatrix} r_1+j\omega L_1 \cdots & j\omega M_{1n} & \cdots j\omega M_{1n+m} \\ | & | & | \\ j\omega M_{n1} \cdots & r_n+j\omega L_n & \cdots j\omega M_{nn+m} \\ | & | & | \\ j\omega M_{n+m1} \cdots & j\omega M_{n+mn} & \cdots r_{n+m}+j\omega L_{n+m} \end{bmatrix}$$

$$\{i\} = [i_1\ i_2 \cdots i_{n+m}]^T, \quad \{e\} = [e_1 \cdots\cdots e_2 \cdots\cdots]^T$$

From Eq. 4, we have

$$\{i\} = [Z]^{-1}\ \{e\} = [Y]\ \{e\} \qquad (5)$$

where the matrix $[Y]$ is the inverse of $[Z]$. Let us consider the series defined by

$$I_1 = \sum_{k=1}^{n} i_k, \qquad I_2 = \sum_{k=n+1}^{n+m} i_k \qquad (6)$$

Now consider that the currents determined by the values I_1 and I_2 are equal to the total current of lead I and lead II.

Then Eq. (5) reduces to

$$\begin{bmatrix} e_1 \\ e_2 \end{bmatrix} = \begin{bmatrix} \sum_{j=1}^{n}\sum_{k=1}^{n} Y_{jk} & \sum_{j=n+1}^{n+m}\sum_{k=1}^{n} Y_{jk} \\ \sum_{j=1}^{n}\sum_{k=n+1}^{n+m} Y_{jk} & \sum_{j=n+1}^{n+m}\sum_{k=n+1}^{n+m} Y_{jk} \end{bmatrix} \begin{bmatrix} I_1 \\ I_2 \end{bmatrix} \qquad \text{--- (7)}$$

Eq. (7) is the Kirchhoff's voltage equation for lead I and lead II. Hence, the high-frequency resistance of lead I R_1 is written in the form

$$R_1 = \mathrm{Re}\left\{\frac{e_1}{I_1}\right\} = \mathrm{Re}\left\{\sum_{j=1}^{n}\sum_{k=1}^{n} Y_{jk} + \sum_{j=n+1}^{n+m}\sum_{k=1}^{n} Y_{jk}\frac{I_2}{I_1}\right\} \qquad \text{--- (8)}$$

Similarly, for lead II,

$$R_2 = \mathrm{Re}\left\{\frac{e_2}{I_2}\right\} = \mathrm{Re}\left\{\sum_{j=1}^{n}\sum_{k=n+1}^{n+m} Y_{jk}\frac{I_1}{I_2} + \sum_{j=n+1}^{n+m}\sum_{k=n+1}^{n+m} Y_{jk}\right\} \qquad \text{--- (9)}$$

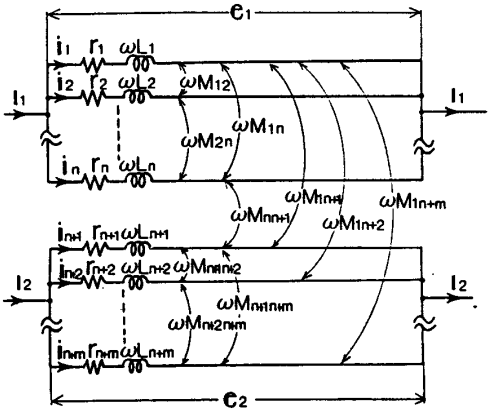

Fig. 4. Equivalent circuit model for two leads.

Table 1: Substituting parameters

Variable	Substituting parameter	Variables	Substituting parameter
x_1	q+c	y_3	p-b
x_2	q	y_4	p+d-b
x_3	q-a	z_1	l_2+l_3
x_4	q+c-a	z_2	l_3
y_1	p+d	z_3	l_3-l_1
y_2	p	z_4	$l_2+l_3-l_1$

Numerical results

The following investigations are performed to confirm the accuracy of this method.

As a test problem, the numerical results are compared with the exact solution of a rectangular conductor, considering the skin effect only[5] . Figure 5 shows the percentage of calculated errors versus changes in mesh width. These results show that, for mesh widths less than skin depth δ, calculations are accurate. The calculation accuracy increases as the mesh width decreases. However, with the floating-point formats of digital computers, this accuracy is not always achievable. If inverse matrix [Z] cannot be solved by a standard FORTRAN program, the manipulating programs [6] must be used.

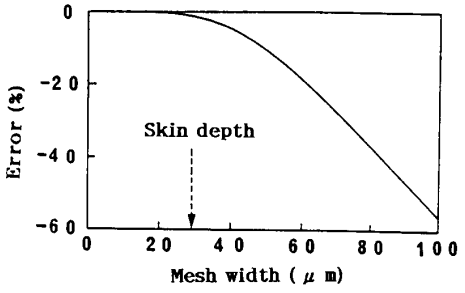

Fig. 5. High-frequency resistance error versus the mesh width for a square lead conductor (200 μ m × 200 μ m) at 5 MHz.

In Figure 6, the skin effect is given for single isolated leads of different conductor shapes. T/w is the ratio of conductor thickness t to conductor width w. Also, Rac / Rdc is the ratio of high-frequency resistance to direct-current resistance. If the ratio of t to w is chosen to be as small as possible, a reduction of high-frequency resistance can be obtained.

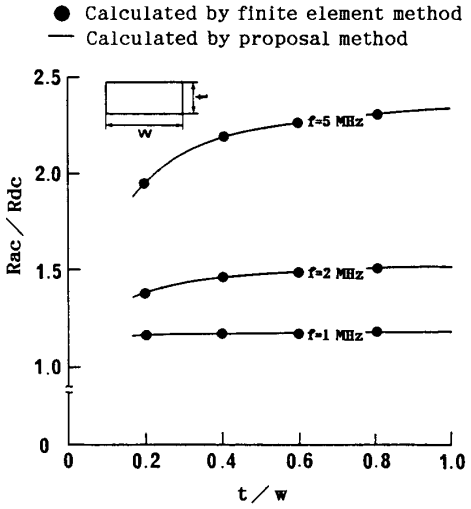

Fig. 6. Skin effect of rectangular lead conductors. Cross-sectional area: 0.04mm^2.

Figure 7 shows the proximity effect for two parallel leads. The independent variable is a distance s of two leads. Rac/R∞ is the ratio of the high frequency resistance, including skin and proximity effects, to the single lead resistance, existing skin effect only. Figure 7 indicates that proximity effect depends to a large extent upon the different distance. Referring figure 7 it is seen that when w/s, where w is a width of the lead, is less than 0.2 the proximity effect is negligible.

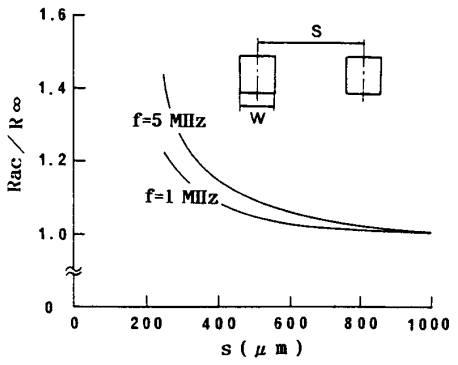

Fig. 7. Proximity effect at w = 200 μ m.

WINDING RESISTANCE

List of symbols

Definitions of symbols used here are as follows.

b: Winding width
h: Winding thickness
d: Diameter of a round conductor
b_w: Winding width
N_ℓ : Number of turns in a layer
m: Number of whole layers
η : Conductor spacing factor ($= \frac{N_\ell b}{b_w}$)
V_p: Voltage drop at the pth layer
I: total current
V: total voltage drop
Rw: Winding high-frequency resistance
i_p: Current at the pth layer
l_{w1}:Turn length of a winding
l_{g1}:Turn length of a gap
u: Height of an interlayer gap

$\alpha : \sqrt{\frac{j\omega\mu_0\eta}{\rho}}$ $\quad j=\sqrt{-1}$

Assumptions

The following are assumed.

(1) Field distribution is uniform and parallel to the solenoidal layers.
(2) If the conductors are round, the equivalent square conductors are derived as b=h=0.886d.

Analysis

The winding resistances of the three different winding constructions shown in Fig. 3 are calculated. From electomagnetic theory and m .m .f. diagrams, the winding resistance equations are derived as follows.

(Multilayer pile winding)

It is shown in Appendix B that the voltage drop in any winding layer can be calculated as follows.

$$V_p = \frac{\rho N \iota^2 \alpha l_{wp}}{\eta b}\{i_p \coth \alpha h + \sum_{k=1}^{p-1} i_k \tanh\frac{\alpha h}{2}\}$$
$$+j\omega \frac{\mu_0 N \iota^2}{b\alpha} \sum_{q=p+1}^{m} l_{wp}(i_q + 2\sum_{k=1}^{q-1} i_k)\tanh\frac{\alpha h}{2}$$
$$+j\omega \frac{\mu_0 N \iota^2}{b\alpha} u \{\sum_{q=p}^{m-1}\sum_{k=1}^{q} l_{gq} i_k + \frac{lgm}{2}\sum_{k=1}^{m} i_k\}$$
$$p=1, 2, 3\text{-----}, m \quad (10)$$

The quantities V_p and i_k may be real or complex numbers. If the relation in Eq. (10) exists between the variables V_p and i_k ($k=1 \sim m$), then the set of variables V_p is said to be derived from the set i_k by a linear transformation. The set of Eq. (10) may be represented by the following single matrix equation.

$$\{V\} = [Z] \{i\} \quad (11)$$

where $\{V\}$ and $\{i\}$ comprise the column matrix, and the square matrix $[Z]$ is the impedance matrix. The elements of $[Z]$ are calculated by Eq. (10).

The current displacement is derived in terms of the voltage.

$$\{i\} = [Z]^{-1}\{V\} = [Y]\{V\} \quad (12)$$

The set of variables V_p are equal, because the winding layers are connected in parallel. Since $V_1=V_2=V_3=\text{-------}=V_m=V$, we have

$$\sum_{p=1}^{m} i_p = I = V\{\sum_{p=1}^{m}\sum_{q=1}^{m} Ypq\} \quad (13)$$

where Ypq is an element of matrix $[Y]$.

Therefore, high-frequency resistance of winding Rw is

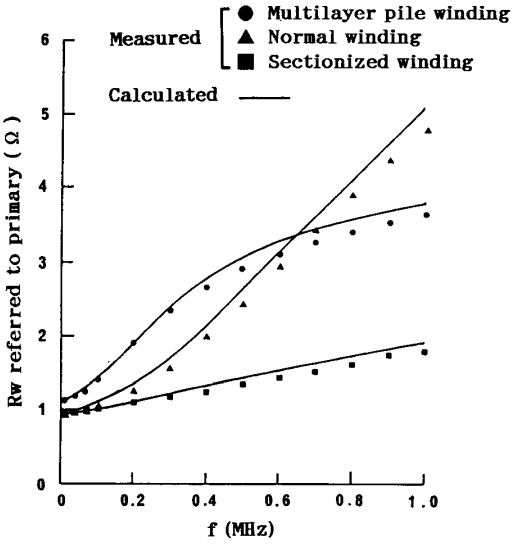

Fig. 8. Winding resistance with changes in winding arrangements.

Core: EQ 9.8 / 9.0 (Ferrite core)
Effective cross-sectoinal area = 10 (mm^2)
Effective magnetic length = 20 (mm)
Windings: Transformer ratio = 1
(For multilayer pile winding)
Coil: ϕ 0.1 mm
N ι : 40
m: 3
(For normal and sectionized windings)
Coil: ϕ 0.19 mm
N ι : 20
m: 2

$$Rw = Re\{\frac{V}{I}\} = Re\{\frac{1}{\sum_{p=1}^{m}\sum_{q=1}^{m} Ypq}\} \quad (14)$$

(Normal winding)

In this winding arrangement, winding currents are equal in magnitude and phase. Hence the set of currents in Eq. (11) satisfies $i_1=i_2=i_3=\text{------}=i_m=I$. We now have

$$\sum_{p=1}^{m} V_p = V = I(\sum_{p=1}^{m}\sum_{q=1}^{m} Zpq) \quad (15)$$

Therefore,

$$Rw=Re\ \{\frac{V}{I}\} =Re\ \{\sum_{p=1}^{m}\sum_{q=1}^{m}Zpq\} \qquad (16)$$

(Sectionized winding)

If the winding contains an even number of layers, it can be split into two portions, and Eq. (16) can be applied to each of the portions.

If the winding contains an odd numbers of layers, each half layer can be considered to be mode of half turns [1] and Eq. (16) may be used.

Experimental results

These results were compared with experimental results. The calculated and measured winding resistance are shown in Fig. 8 and Fig. 9 respectively. The values agree well. At high frequencies, sectionized winding can be used to reduce winding resistance. However, increasing the number of layers is not effective in reducing winding resistance in multilayer pile windings.

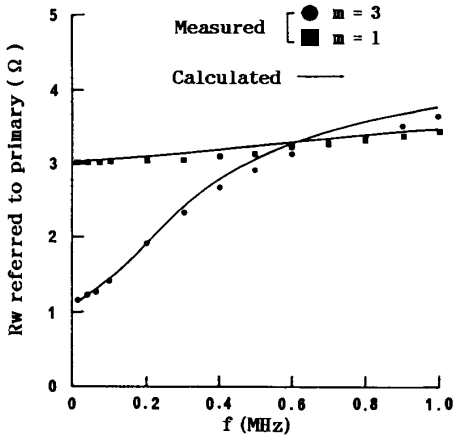

Fig. 9. Winding resistance with changes in the number of layers connected in parallel.

Core: EQ9.8 / 9.0
Windings: Transformer ratio = 1
Coil: ϕ 0.1 mm
N ℓ : 40

CONCLUSION

A new method for calculating the lead and winding high-frequency resistance of transformers was presented. The mathematical procedure, which solves the resulting matrix system equation, common to the lead and winding, was discussed. This procedure enables exact calculation of high-frequency resistance of complex geometries. Calculations were presented with theoretical and experimental data on corresponding geometries.

Finally, three different winding constructions were evaluated.

ACKNOWLEDGMENT

The authors would like to thank Katsuichi Yotsumoto and Toshiyuki Sugiura for their helpful comments.

REFERENCES

[1] P. L. Dowell, "Effects of Eddy Currents in Transformer Windings", PROC. IEE, No. 8, August 1966, pp. 1387-1966.

[2] E. C. Snelling, SOFT FERRITES, Butterworth & Co., 1988, chap. 11.

[3] A. F. Goldberg, J. G. Kassakian,and M. F. Schlect, "Finite Element Analysis of Copper Loss in 1-10MHz Transformers", PESC' 88 Rec., April 1988, pp. 1105-
1111.

[4] C. Hoer, et al., "Exact Inductance Equations for Rectangular Conductors with Applications to More Complicated Geometries", J. Res, NBS-69C, 1965,pp. 127-137.

[5] H. B. Dwight, "Skin Effect in Tubular and Flat Conductors", A. I. R. E., 1918, pp. 1379-1403.

[6] IBM, IBM High-Accuracy Arithmetic Subroutine Library, GC33-6163-02, 1986.

APPENDIX

A. Representation of the function $f(x_i,y_i,z_k)$

Hoer presented inductance equations taking into consideration the geometric mean distance between rectangular bars [4] . These equations can be used to calculate exact the inductance for the bars which have relatively large cross-sectional areas. These equations, which can be seen by writing Eq. 2 in the form and function $f(x_i,y_i,z_k)$, are given by

$$f(x_i,y_i,z_k)=\left(\frac{y_j^2z_k^2}{4}-\frac{y_j^4}{24}-\frac{z_k^4}{24}\right)x_i\log\left(\frac{x_i+A}{\sqrt{y_j^2+z_k^2}}\right)$$

$$+\left(\frac{z_k^2x_i^2}{4}-\frac{z_k^4}{24}-\frac{x_i^4}{24}\right)y_j\log\left(\frac{y_j+A}{\sqrt{x_i^2+z_k^2}}\right)$$

$$+\left(\frac{x_i^2y_j^2}{4}-\frac{x_i^4}{24}-\frac{y_j^4}{24}\right)z_k\log\left(\frac{z_k+A}{\sqrt{x_i^2+y_j^2}}\right)$$

$$+\frac{1}{60}(x_i^4+y_j^4+z_k^4-3x_i^2y_j^2-3y_j^2z_k^2-3z_k^2x_i^2)A$$

$$-\frac{x_i^3y_jz_k}{6}\tan^{-1}\left(\frac{y_jz_k}{x_iA}\right)-\frac{x_iy_j^3z_k}{6}\tan^{-1}\left(\frac{z_kx_i}{y_jA}\right)$$

$$-\frac{x_iy_jz_k^3}{6}\tan^{-1}\left(\frac{x_iy_j}{z_kA}\right) \qquad \text{(A1)}$$

where A is $\sqrt{x_i^2+y_j^2+z_k^2}$.

B. Pth layer voltage drop

Dowell derived voltage induced by the flux crossing the pth layer and the resistive voltage across a layer at the tops of conductors[1] . The qth layer flux induces a voltage Viq in each of the (q-1) lower layers. Thus the induced voltage drop Vfp due to the flux over the pth layer is

$$Vfp=\sum_{q=p+1}^{m} Viq \qquad \text{(A2)}$$

The pth layer voltage drop is the sum of Eq. (A2) and the resistive voltage, as shown in[1] .